Compact Mach-Zehnder acousto-optic modulator

M. M. de Lima, Jr.,[a] M. Beck, R. Hey, and P. V. Santos
Paul-Drude-Institut für Festkörperelektronik, Hausvogteiplatz 5-7, 10117 Berlin, Germany

(Received 22 May 2006; accepted 4 July 2006; published online 19 September 2006)

The authors demonstrate a compact optical waveguide modulator based on a Mach-Zehnder interferometer driven by surface acoustic waves. The modulator was monolithically fabricated on GaAs with an active region length of approximately 15 μm. It yields peak-to-peak modulation exceeding 90% of the average transmission and operation in the gigahertz frequency range. © *2006 American Institute of Physics*. [DOI: 10.1063/1.2354411]

Acousto-optic effects have been used for optical modulation for a long time, with the Bragg cells being probably the best known example.[1] The demand for fast and compact devices together with required phase matching, however, imposes several limitations on conventional acousto-optic devices in future generations of integrated photonics. Therefore, great attention has recently been devoted to alternative concepts for light modulation. A promising approach to increase the operation speed employs all-optical light control, which allows operation down to the subpicosecond time scales.[2] These devices are typically a few hundreds of microns long since they rely on optical nonlinearities that are usually small. An effective approach to reduce device dimensions employs photonic crystals (PhCs). Examples are thermo-optical switches based on a PhC Mach-Zehnder interferometer (MZI) with 12-μm-long arms on AlGaAs/GaAs system[3] as well as electro-optical switches based on carrier injection of 80-μm-long silicon PhC-MZI.[4] In both cases the switching time is on the order of microseconds. Faster PhC-based all-optical switching devices have been realized in the (Al,Ga)As system by taking advantage of the nonlinear properties of quantum dots embedded in the MZI arms.[5] PhC fabrication, however, requires a sophisticated technology with very strict tolerances.

In this letter, we demonstrate a compact and monolithic modulator based on conventional ridge waveguides (WGs) on GaAs. The modulator consists of a MZI driven by a surface acoustic wave (SAW) in the gigahertz range, where the length of the interaction region between the acoustic and optical waves (the active region) is reduced to approximately 15 μm. The design used, which is a modified version of the acousto-optic MZI proposed by Gorecki *et al.*,[6] is based on the refractive index modulation of the interferometer arms by the wave fronts of a SAW propagating perpendicularly to the arms. The changes in refractive index are induced by the elasto-optic and electro-optic effects associated with the strain and piezoelectric fields, respectively. For photon energies away from electronic transitions—which is the case discussed here—the elasto-optical effect dominates.[7] The width of the WGs forming the arms is chosen to be much smaller than the acoustic wavelength (λ_{SAW}) in order to ensure a constant modulation amplitude across the WG width. In our design, we introduce two fundamental modifications to increase the modulation efficiency and reduce the length of the active region. First, we enhance the modulation efficiency by modulating simultaneously both interferometer arms using the same SAW (in the original proposal,[6] only one of the arms is modulated). For that purpose, the MZI arms are separated by an odd multiple of $\lambda_{SAW}/2$, in order to experience refractive index changes of opposite phase during the passage of the SAW. The second modification consists in using a focusing interdigital transducer (IDT) to generate a narrow and strong acoustic beam.

The devices were fabricated on a WG sample grown by molecular beam epitaxy on a GaAs (100) wafer [see Fig. 1(a)]. The sample consists of a 300-nm-thick GaAs film

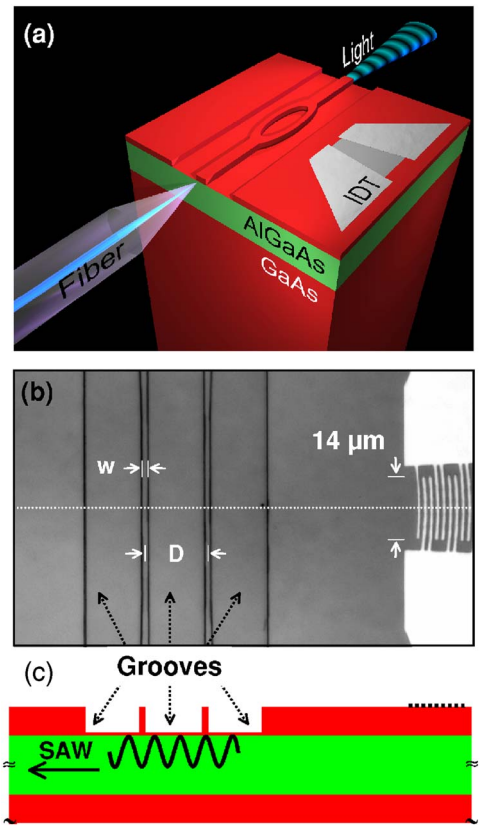

FIG. 1. (Color online) (a) Schematic view of the MZI modulated by a surface acoustic wave (SAW). The incoming light is coupled into the device by a tapered fiber, while the modulated outgoing light is detected at the opposite cleaved edge. The SAW is generated by a focusing interdigital transducer (IDT) operating at a wavelength $\lambda_{SAW}=5.6$ μm and frequency $f_{SAW}=520$ MHz. (b) Optical micrograph with a top view of the MZI active area. The ridge waveguides forming the MZI arms with width $w=1.4$ μm are spaced by $D=2.5\lambda_{SAW}=14$ μm to experience opposite phases of the acoustic field, as illustrated in the cross-section view in (c).

[a]Electronic mail: mmlimajr@pdi-berlin.de

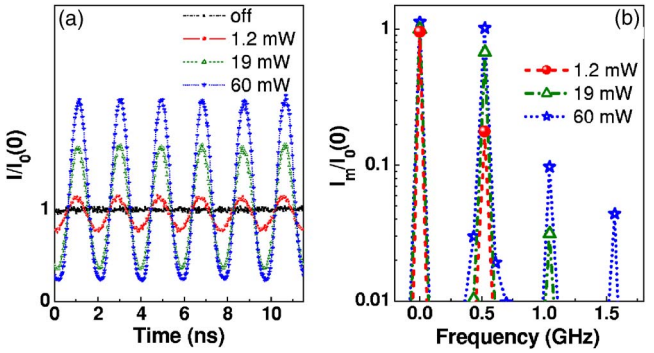

FIG. 2. (Color online) (a) Measured time-resolved light transmission (I) through the MZI for different acoustic powers (P_{IDT}), normalized to the value transmitted in the absence of a SAW [$I_0(0)$]. (b) Fourier transformation (with components I_m) of the transmitted intensity of the data displayed on (a).

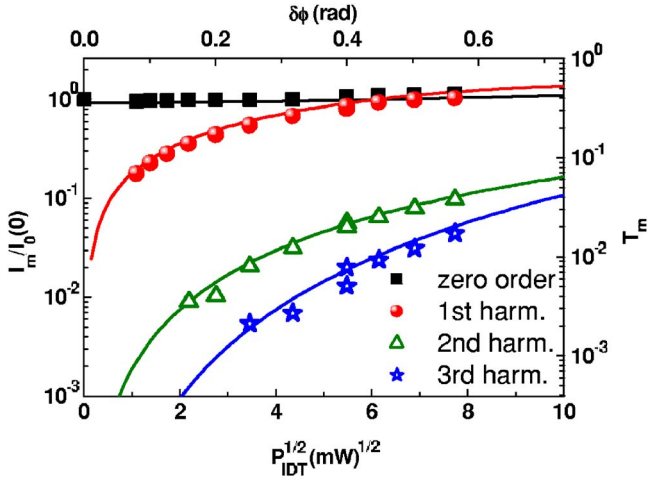

FIG. 3. (Color online) Amplitude of the mth-order harmonic of the transmitted intensity [$I_m(P_{\mathrm{IDT}})$] as a function of $\sqrt{P_{\mathrm{IDT}}}$ (symbols), normalized to the average transmission in the absence of a SAW [$I_0(0)$]. The solid lines are calculated from Eqs. (1)–(4) with $\delta\phi_s=0.927$ rad as the only adjustable parameter. The upper and right axes display the amplitude of the phase shift modulation $\delta\phi$ and the calculated absolute transmission coefficient for the mth harmonic, respectively.

forming the core of the surface WG deposited on a 1500-nm-thick $Al_{0.2}Ga_{0.8}As$ cladding layer. The MZI was fabricated in two steps using contact optical lithography: the fabrication of the IDTs for SAW generation using a lift-off process to structure the 60-nm-thick metal layer followed by the plasma etching of the 280-nm-deep grooves delimiting the ridge WGs of the MZI. The focusing IDTs were designed for an operation wavelength $\lambda_{\mathrm{SAW}}=5.6$ μm (corresponding to a resonance frequency of approximately 520 MHz) following the procedure discussed in detail in Ref. 8. These IDTs generate a SAW beam with full width at half maximum $\ell \approx 15$ μm that are collimated over hundreds of microns. A crucial feature in the design is the separation (D) between the MZI arms [see Figs. 1(b) and 1(c)], which was chosen to be $D=2.5\lambda_{\mathrm{SAW}}$. The width of the WGs within the active region was $w=\lambda_{\mathrm{SAW}}/4=1.4$ μm. While narrow enough to prevent the smearing of the modulation, this width is sufficient for reliable fabrication using optical lithography and etching techniques. The additional WGs connecting the light to the MZI arms (including the input and output WGs as well as the Y branches) were 10 μm wide. Although this configuration leads to an overall multimode behavior of the interferometer, individual modes can be spatially filtered.

The devices were optically characterized by coupling light into the input WG using a tapered fiber with a cylindrical lens on its tip [see Fig. 1(a)]. As light source, we used a superluminescent diode with peak emission centered at the wavelength $\lambda=950$ nm with a full width at half maximum of approximately 50 nm. The fiber was mounted on a piezoelectrically controlled stage in order to allow for a fine positioning relative to the WG edge. Due to its multimode character, the mode configuration excited within the MZI becomes controlled by the position of the input fiber. The transmitted light was collected using a $2\times$ microscope objective focused on the cleaved edge of the output WG. The small numerical aperture of this objective allows us to select the far-field emission of individual modes leaving the WG. The light was then detected with a time resolution of 500 ps using a Si avalanche photodiode synchronized with the rf signal driving the IDTs.

Time-resolved transmission traces recorded for different rf powers (P_{IDT}) coupled to the IDT are shown in Fig. 2(a) for light with TE polarization. P_{IDT} was determined taking into account the IDT reflection losses measured using a network analyzer. Note that due to the bidirectionality of the IDT, the acoustic power modulating the MZI arms corresponds to only half of P_{IDT}. The light coupling conditions in Fig. 2(a) were chosen to yield a strong modulation at the fundamental SAW frequency. Oscillations of the transmitted light intensity with the SAW period and with amplitude increasing with P_{IDT} are observed. For the highest acoustic power ($P_{\mathrm{IDT}}=60$ mW), the modulation amplitude becomes comparable to the average transmission in the absence of acoustic excitation. The oscillations are asymmetric in this case, thus indicating the presence of higher harmonics. These harmonics become evident in the Fourier transformation of the data of Fig. 2(a) displayed in Fig. 2(b). Here, the transmission intensity (I_m) modulated at the mth harmonic of the SAW frequency has been normalized to the intensity $I_0(0)$ in the absence of acoustic excitation. Transmission up to the third harmonic of the SAW frequency is clearly observed: the detection of higher harmonics (with frequencies >2 GHz) is prevented by the limited time resolution of the experimental setup. In agreement with the previous discussion, the amplitude of the first harmonic T_1 exceeds 90% of the continuous transmission T_0 for $P_{\mathrm{IDT}}=60$ mW.

Two checks were carried out to verify that the observed light modulation is indeed caused by the opposite phase changes imposed by the SAW on the two arms of the MZI. In the first, we measured the transmission through a single WG with a width identical to those in the MZI. In the second check, the separation D between the arms [see. Fig. 1(b)] was changed to $D=3\lambda_{\mathrm{SAW}}$ so as to make the phase of the acoustically induced refractive index changes equal for both arms. In both cases, the refractive index modulation by the SAW leads to a modulation of light transmission. The measured modulated amplitudes, however, were found to be at least 20 times smaller than for the MZI with $D=2.5\lambda_{\mathrm{SAW}}$.

Further information about the modulation mechanisms has been obtained from detailed measurements of the rf power dependence of the transmitted intensities I_m illustrated in Fig. 3, which were recorded under coupling conditions identical to those of Fig. 2. The transmission intensities for $m=0,\ldots,3$ are again normalized to the average (i.e., time

integrated) transmission in the absence of a SAW $[I_0(0)]$. The results are plotted as a function of the square root of the applied rf power (lower horizontal axis) to emphasize the fact that the light phase changes induced by the SAW $[\delta\phi = (2\pi\ell/\lambda)\delta n$, where δn is the average amplitude of the SAW-induced refractive index modulation in the active region $\ell]$ are proportional to the strain field and, therefore, $\delta\phi = a_P\sqrt{P_{\mathrm{IDT}}}$. The proportionality constant $a_P \approx 7.3 \times 10^{-2}\mathrm{rad}/\sqrt{\mathrm{mW}}$ was determined from the IDT geometry and from calculations of the depth profile of the SAW field, which were carried out following the procedure described in Ref. 7.

In order to calculate the optical modulation, we assume that the interferometer arms experience small phase shifts of opposite phases with amplitude given by $\Delta\phi = \delta\phi\cos(\omega_{\mathrm{SAW}}t)$. For each light mode, the transmission coefficient T_m for the light modulated at frequency $m\omega_{\mathrm{SAW}}$ becomes

$$T_0 = \frac{1}{2}[1 + \cos(2\delta\phi_s)J_0^2(\delta\phi)] - [J_1^2(\delta\phi) - J_2^2(\delta\phi)]\cos(2\delta\phi_s), \quad (1)$$

$$T_1 = -2J_1(\delta\phi)[J_0(\delta\phi) - J_2(\delta\phi)]\sin(2\delta\phi_s), \quad (2)$$

$$T_2 = [J_1^2(\delta\phi) + 2J_0(\delta\phi)J_2(\delta\phi)]\cos(2\delta\phi_s), \quad (3)$$

$$T_3 = -2J_1(\delta\phi)J_2(\delta\phi)\sin(2\delta\phi_s), \quad (4)$$

where J_m is the Bessel function of order m. The parameter $\delta\phi_s$ describes the *static* phase shift associated with the asymmetry between the arms. In our multimode design, $\delta\phi_s$ depends on the mode excited within the interferometer, which can be controlled by varying the position of the tapered fiber.

The solid lines in Fig. 3 show a fit of Eqs. (1)–(4) to the experimental data using as fit parameter the static phase shift $\delta\phi_s$, which was determined to be $\delta\phi_s = 0.927$ rad. The fits yield $\delta\phi$ and the transmission coefficients T_m, which are plotted in the upper and right axes of Fig. 3, respectively. $\delta\phi_s$ is close to $\pi/4$, thus ensuring a strong modulation at the first harmonic of the SAW frequency [see Eq. (2)] for the chosen experimental conditions. The calculations reproduce remarkably well the power dependence of the transmission factors. Note that for the highest rf power one achieves phase shifts $\delta\phi$ close to $\pi/5$ per arm.

In summary, we have realized an acoustically driven ultra compact waveguide modulator based on a Mach-Zehnder interferometer driven by a surface acoustic wave. Peak-to-peak modulation amplitudes exceeding 90% of the average transmission have been achieved together with modulation up to the third harmonic at 1.56 GHz. The modulation concept described here can easily be extended to nonpiezoelectric material systems, such as Si, by depositing a piezoelectric overlayer.[6] Finally, from a technological point of view it should be possible to scale down the device dimensions, leading to higher operation frequencies and shorter active region lengths.

The authors thank K. H. Ploog and M. Ramsteiner for comments and for a critical reading of this letter. They also thank M. Höricke, H. Kostial, A. Scheu, W. Seidel, and E. Wiebicke for preparation of the devices. Support from the EU Network of Excellence ePIXnet is gratefully acknowledged.

[1] A. Korpel, *Acousto-Optics* (Dekker, New York, 1997), p. 35.
[2] S. Nakamura and K. Tajima, Jpn. J. Appl. Phys., Part 2 **35**, L1426 (1996).
[3] E. A. Camargo, H. M. H. Chong, and R. M. De La Rue, Opt. Express **12**, 588 (2004).
[4] Y. Jiang, W. Jiang, L. Gu, X. Chen, and R. T. Chen, Appl. Phys. Lett. **87**, 221105 (2005).
[5] Y. Tanaka, Y. Sugimoto, N. Ikeda, H. Nakamura, K. Kanamoto, K. Asakawa, and K. Inoue, Appl. Phys. Lett. **86**, 141104 (2005).
[6] C. Gorecki, F. Chollet, E. Bonnotte, and H. Kawakatsu, Opt. Lett. **22**, 1784 (1997).
[7] M. M. de Lima, Jr. and P. V. Santos, Rep. Prog. Phys. **68**, 1639 (2005).
[8] M. M. de Lima, Jr., F. Alsina, W. Seidel, and P. V. Santos, J. Appl. Phys. **94**, 7848 (2003).